

# p-n Junctions in Silicon Nanowires

G. GONCHER,<sup>1</sup> R. SOLANKI,<sup>1,3</sup> J.R. CARRUTHERS,<sup>1</sup> J. CONLEY, JR.,<sup>2</sup>  
and Y. ONO<sup>2</sup>

1.—Department of Physics, Portland State University, Portland, Oregon. 2.—Sharp Laboratory of America, Camas, Washington. 3.—E-mail: solanki@csee.ogi.edu

Silicon nanowires composed of p-n junctions have been grown on  $2 \times 5$  cm glass substrates with a thin layer of indium tin oxide (ITO). These nanowires were grown both directly on ITO utilizing the vapor–solid (VS) method, as well as by vapor–liquid–solid (VLS) method, with a thin layer of gold as a catalyst. Current–voltage analyses show p-n diode characteristics in both cases. When a reverse dc bias was applied, these diodes responded to optical signals incident on the glass surface, showing potential solar-cell application and intriguing possibilities for future optical detection structures. Devices grown via the VS method displayed better electrical properties compared to those produced via the VLS method.

**Key words:** Silicon, nanowires, diode

## INTRODUCTION

Over the past few years, it has become evident that the trend of continued down-scaling of silicon integrated circuits to increase speed is reaching its limit. To continue the trend predicted by Moore's Law, new nanoscale device structures will be required to overcome the physical limitations of overlapping electrical fields and current leakage of the two-dimensional field-effect transistors. One possible solution to overcome these limitations is use of silicon nanowires (SNWs), which can potentially produce one-dimensional (1-D), single-crystal structures for fabrication of future electronic and optoelectronic devices. The motivation of utilizing 1-D channels stems from the possibility of achieving coherent or quantum transport of carriers. Semiconductor nanowires, in particular SNWs, are particularly attractive because their electrical conduction can be predictably controlled by doping. To date, doped individual SNWs have been utilized to demonstrate a wide range of devices, ranging from field-effect transistors to biosensors.<sup>1–4</sup> The NWs in these devices were grown either by laser ablation or the vapor–liquid–solid (VLS) method, with Au as the catalyst in both methods.<sup>5,6</sup> However, Au in contact with Si leads to deep-level traps in Si; hence this combination is avoided in the microelectronics industry. Therefore, we have explored other methods, particularly the vapor–solid (VS) method of growing SNWs which does not require Au.<sup>7</sup> We present below our results of growth of p-n junctions in SNWs grown

by VS and VLS methods, for comparison. The NWs were grown on glass substrates for large-area applications, such as solar cells. The optical sensitivity of these devices also opens up the possibility of using these structures for fabricating charge-coupled devices (CCDs) and avalanche photodiodes (APDs).

## EXPERIMENTAL DETAILS

In the VS method, control of degree of supersaturation is critical because it determines the morphology of the deposition.<sup>7</sup> For growth of NWs, low supersaturation of the vapor-phase source is required, whereas increasing it leads to deposition of a film. In order to meet this condition, selection of an appropriate source is important. We found disilane to be a suitable source for this method as it decomposes at about 410°C and has two Si atoms per molecule, therefore producing the necessary supersaturation at relatively low temperatures. The substrates for the SNW growth consisted of 2 cm  $\times$  5 cm glass (Corning 7059, Corning, NY) plates with a thin (200 nm) polycrystalline film of indium tin oxide (ITO). ITO is a transparent conductor that is commonly used as the front electrode in displays and solar cells. It has a work function in the range of 4.60–4.75 eV, depending on the processing conditions, hence it has also been utilized for injecting holes into organic semiconductors.<sup>8,9</sup> For VLS growth, the ITO surface was covered with a 1–2 nm thick Au film or 10-nm diameter Au nanoparticles.

The SNW growth was carried out in a quartz reactor that was placed in a horizontal furnace. The flow rate of the source gases was controlled with

Volu  
PAGE  
1509  
1513  
1518  
1523  
1530  
1537  
1543  
1547  
1552  
1558  
1566  
1571  
1581  
1593  
1600  
L7

electronic flow meters. Further details of the growth system are presented elsewhere.<sup>10</sup> The source of Si was disilane (10%, balance Ar). Initially, diborane ( $B_2H_6$ ) was used as a B source to produce p-type doping. After a series of growth parameters were tested to optimize the doping conditions, the best that we could produce were short, stubby wires. This is probably due to a gas-phase catalytic reaction similar to that which occurs between  $B_2H_6$  and silane that leads to an increase in deposition rate of Si.<sup>11</sup> We then switched the B source to trimethylboron (TMB), which has been reported to produce controllable B-doping of SNWs.<sup>12</sup> This source allowed B-doping of SNWs over a relatively large range of B concentration and did not seem to affect the NW morphology over the temperature range examined. The source for n-type doping was phosphine ( $PH_3$ ), which was relatively stable over the temperature range used for the NW growth. The starting concentrations of the dopant sources were 100 ppm TMB in  $H_2$  and 100 ppm  $PH_3$  in Ar.

The flow rates of disilane, TMB, and  $PH_3$  were adjusted so that B/Si and P/Si inlet gas ratios were in the  $10^{-3}$  range. Total reactor pressure during growth was about 2 torr, and the temperature was 420°C for VLS (ITO with Au) and 440°C for VS (plain ITO). The growth process was started with first introducing disilane and TMB into the reaction chamber to produce SNWs with p-type ends in contact with ITO. The growth continued for 10 min. ( $\sim 1 \mu m$  NW length). The TMB flow was turned off,  $PH_3$  was introduced into the reactor, and growth continued for another 40 min. ( $\sim 4 \mu m$ ). The reason for keeping the p-type section of the NW short will be apparent later. We estimated the NW density to be  $\sim 10^{10} cm^{-2}$ , and the diameters of the NWs grown were in the 40–50 nm range. This distribution in diameters should result in a corresponding spread in their properties. These substrates were next placed in an atomic layer deposition (ALD) reactor to deposit a 0.4- $\mu m$ -thick layer of  $SiO_2$  at 230°C. ALD allows deposition of a very conformal film around the NWs and fills the gaps between them. Details of ALD of  $SiO_2$  is presented elsewhere.<sup>13</sup> Because ALD fills the gaps between the high density of NWs, a thick film is not required.<sup>14</sup> Next, the  $SiO_2$  layer was etched back in several stages in dilute (10%) HF. Etching was stopped when the tips of the NWs were visible with a scanning electron microscope (SEM). The final step consisted of sputter depositing Al dots 500  $\mu m$  to 2 mm in diameter, followed by a short (30 sec) anneal at 450°C in forming gas (10%  $H_2$ , balance Ar). The Al dots formed the back electrodes. Therefore, the active p-n sandwich structure consisted of ITO/p-Si/n-Si/Al.

### NANOWIRE GROWTH MECHANISMS

As stated before, two growth mechanisms were examined to produce p-n junctions in SNWs. Currently, the most common method utilized to grow SNWs is VLS. In this technique, a thin film or nano-

particles of mostly Au are used to first catalytically decompose the Si source molecule at a temperature higher than the Si-Au eutectic temperature ( $\sim 360^\circ C$ ). Further decomposition of the Si source will increase the Si composition in the eutectic, which will return to equilibrium by precipitating out excess Si in the form of a nanowire. In this growth process, there are two possible ways of incorporating the dopants into the nanowires. Gold does not form a eutectic with B or P.<sup>15</sup> However, it is possible that these dopant atoms are incorporated into the eutectic and precipitated out together with Si. The other possibility is diffusion of the dopants into the NWs through the sidewalls. Based on diffusivities of B and P in Si<sup>16</sup> at a growth temperature of 450°C and time of 30 min., we estimated the diffusion lengths of boron to be  $\sim 3 \times 10^{-13}$  m and about half of this for phosphorous. Hence, the latter doping mechanism is less likely. Also, if this mechanism were significant, then it would have made formation of longitudinal p-n junctions in NWs virtually impossible, because the second dopant would also penetrate into the previously doped region.

The second growth mechanism we examined was vapor-solid, where the growth surface was ITO, without any Au. Except for a slightly higher temperature (440°C), all other growth parameters were the same as for the VLS case. Once nucleated, a NW grows by further decomposing the source gases at the free end, where the dopants are apparently incorporated. At this time it is not clear which thermodynamic mechanisms lead to the source gas(es) decomposing at the free end and incorporation of the dopants. Transmission electron microscopy (TEM) analysis of undoped SNWs using energy-dispersive x-ray spectroscopy (EDS) have shown no detectable levels of either In or Sn from ITO (results to be published separately). We have applied this method successfully to grow SNWs on other substrates than ITO, such as mica.

### RESULTS

To determine the doping levels, several sets of NWs were grown, some with B or P alone and others with p-n junctions. Samples consisting of B- or P-doped NWs (grown under the same conditions as the p-n junctions) were first characterized using time-of-flight secondary ion mass spectroscopy (TOFSIMS). In the case of B-doped NWs, initially small signals of silicon and oxygen were detected, corresponding to a layer of native oxide. These peaks were followed by steady signals of silicon and boron. The boron concentration was  $5 \times 10^{20} cm^{-3}$ , which was consistent over several areas probed. There was no significant amount of B on the surface. Similarly, in the case of P-doped SNWs, the phosphorous concentration was determined to be  $3.4 \times 10^{19} cm^{-3}$ . This technique does not provide doping information of an individual NW but rather an average of several wires. NWs with p-n junctions were also examined with a STEM, where several of them were

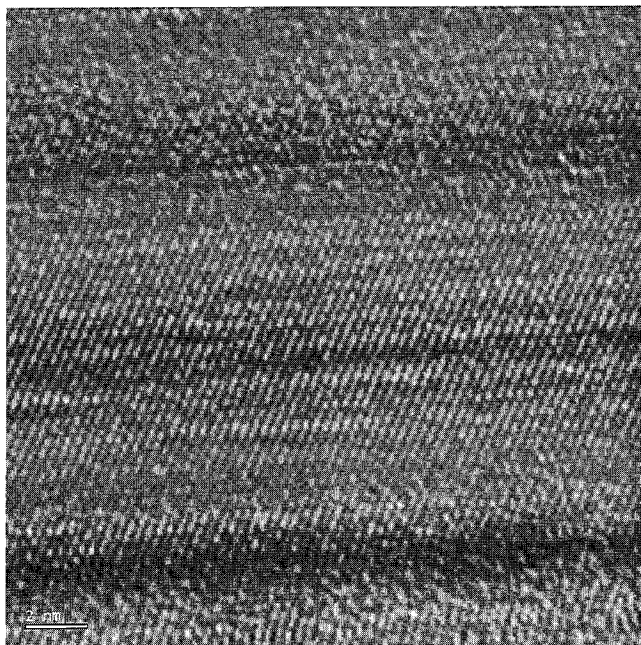


Fig. 1. High-resolution TEM view of P-doped cross-section of the silicon nanowire.

individually probed along their length for B and P using EDS. P was detected at a concentration of about  $3 \times 10^{18} \text{ cm}^{-3}$ . A high-resolution TEM view of a section of P-doped SNW is shown in Fig. 1. One can see that there are no visible defects observable at this doping concentration. Along the length of a NW, P was detected up to a certain length and then it dropped below the sensitivity of the instrument over the rest of the length. In the B-doped region, no B was detected, which was not surprising because EDS is known to have a limitation for sensing light elements. Still in the STEM mode, an alternate technique known as electron energy-loss spectroscopy (EELS) was employed to detect B. Although we could detect B in the section of NWs where it was supposed to be, it was not possible to quantify its concentration.

Electrical response of these SNWs with p-n junctions were characterized with an HP-4145B analyzer. A typical I-V curve of a junction grown by the VS method is shown in Fig. 2 (solid line), which shows a standard diode characteristic. Note that the response shown is a composite of several NWs under the Al electrode. Also note that, in Fig. 2, the driving voltage is rather high for these NW structures. This is caused by the contact to the ITO layer being made at the edge of these devices, and the current had to pass through about 1 cm of this slightly resistive layer. The response of devices grown via VLS is also shown in Fig. 2 (narrow line). The current of the VLS-grown device was multiplied by 4 in order to show its profile on the same plot as the VS-grown device. The I-V curves of these devices were not as smooth, had high resistance, and often tended to break down at lower voltages. It is not obvious that presence of Au is responsible for this behavior in

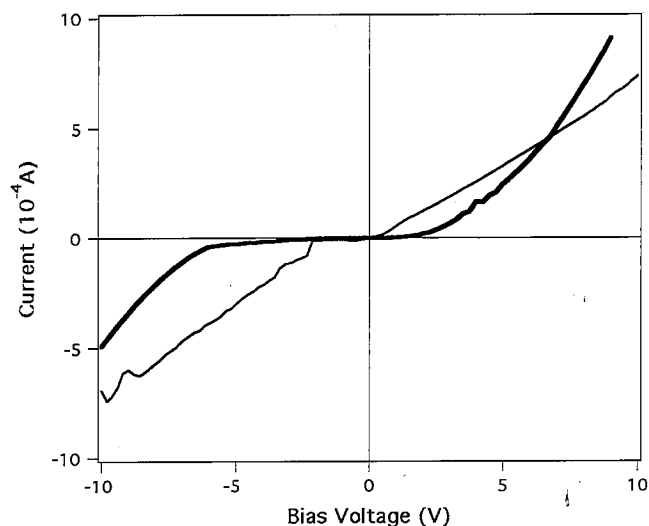


Fig. 2. I-V curves of the p-n junctions grown via VS (wide line) and VLS (narrow line) methods.

these devices, because near-ideal I-V response from VLS-grown SNW with Au as a catalyst has been reported.<sup>17</sup> Hence, it is possible that this behavior is due to our conditions for the VLS growth not being optimum.

It can be argued that the I-V profiles recorded are due to thermionic emission currents of two back-to-back Schottky diodes formed at the SNW-metal junctions. To address this, we examined each contact separately. First, p-type SNWs were grown on ITO using the VS technique. The I-V curves showed a little nonlinearity, but there was no threshold voltage for the current flow. The n-type SNWs were grown on heavily doped ( $\sim 10^{20} \text{ cm}^{-3}$ ) P-doped Si substrates. Au nanoparticles were used as catalysts, employing the VLS method to achieve the NW growth. In this case the I-V curves were ohmic. In both cases, Al was used as the back electrode. Hence, the diode characteristics we observe most likely originate at the p-n junction in the SNWs.

The optical response of these diodes was examined by applying a reverse dc bias and illuminating them with a pulsed light source. The signal produced was viewed on an oscilloscope, as shown in Fig. 3. The light source was an Ar laser operating at 514.5 nm, attenuated to 3  $\mu\text{W}$ , passed through a chopper, and defocused to a beam size of about 5 mm. The light beam was incident on the glass side of the diode. The p-n junction was kept close to the glass substrate (by keeping p-Si segments short) to maximize photocarrier generation, which enhanced the photodiode signal. The dc bias was typically between 4 and 5 V.

Several issues regarding doping of Si nanowires remain to be addressed. For example, although we can see presence of dopants in the NWs, we do not know what fraction of these dopants are activated. To examine this, several samples were annealed at 650°C for 1 min. presence of forming gas, just after NW growth. In all cases, the I-V profiles degraded. This could be due to out-diffusion of the dopants.

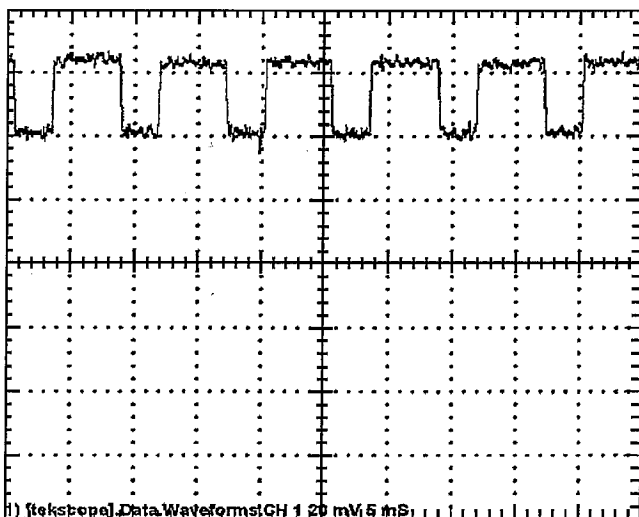


Fig. 3. Optical response of a reverse-biased nanowire p-n junction monitored on an oscilloscope. Horizontal and vertical scales are 5 msec/div. and 20 mV/div., respectively.

The other issue is segregation of dopants at the Si/oxide interface. When doped Si is oxidized, the dopant could preferentially segregate in Si or the oxide.<sup>18</sup> This could present a problem when these NWs undergo thermal cycles during device fabrication. For example, suppose during the device fabrication process, these NWs experience a total temperature of 800°C for 30 min. in dry oxygen. Using SILVACO simulation, we determined that growth of an oxide layer on the NW during this temperature cycle will lead to depletion of B concentration by an order of magnitude at the interface. In the case of n-SNWs, under the same conditions, the P concentration will increase by about 40%.

### SUMMARY

In summary, we have demonstrated large area growth of 40–50 nm diameter Si NWs that are doped longitudinally to produce p-n diodes. The NWs grown using the VS method displayed superior properties compared to those grown via the VLS method, where Au was used as a catalyst. These structures display typical diode I–V characteristics and respond to optical signals, which raise intriguing possibilities for solar cell as well as future CCD and APD applications. Besides p-n junctions, one should be able to extend this process to produce p-i-n structures. Although we have demonstrated the feasibility of fabricating large areas of NWs with p-n junctions, the unique advantage of these nano-

scale structures will be realized only when the Si NW diameters are <5 nm.<sup>19,20</sup> At this scale, Si should have a direct bandgap and the carriers within the NWs will be transported by quantum conductance.

### ACKNOWLEDGEMENTS

The authors thank Dr. Stephen Golledge of CAMCOR Surface Analytical Facility at the University of Oregon, ONAMI for the TOFSIMS analysis, and Prof. Jack McCarthy of OHSU for assistance with TEM analysis. The authors also acknowledge helpful suggestions and discussions with Dr. Marko Radosavljevic of Intel Corporation during the duration of this project. This work was funded in part by Intel Corporation and Sharp Laboratories of America.

### REFERENCES

1. Y. Cui and C.M. Lieber, *Science* 291, 851 (2001).
2. Y. Cui, Q. Wei, H. Park, and C.M. Lieber, *Science* 293, 1289 (2001).
3. H.F. Wang, M.S. Gudiksen, X.F. Duan, Y. Cui, and C.M. Lieber, *Science* 293, 1455 (2001).
4. F. Potolsky and C.M. Lieber, *Mater. Today* 20 (April 2005).
5. Y. Cui, X. Duan, I. Hu, and C.M. Lieber, *J. Phys. Chem. B* 104, 5213 (2000).
6. R.S. Wagner and W.C. Ellis, *Appl. Phys. Lett.* 4, 89 (1964).
7. W.B. Campbell, *Whisker Technology*, A.P. Levitt, ed. (New York: Wiley-Interscience, 1970), pp. 15–45.
8. N. Balasubramanian and A. Subramanyam, *J. Electrochem. Soc.* 138, 322 (1991).
9. C.W. Tang and S.A. Van Slyke, *Appl. Phys. Lett.* 51, 913 (1987).
10. C.A. Decker, R. Solanki, J. Freeouf, J.R. Carruthers, and D.A. Evans, *Appl. Phys. Lett.* 84, 1389 (2004).
11. G. Harbecke, L. Krausbauer, E.F. Stegmeier, A.E. Widmer, H.F. Kappert, and G. Wengebauer, *J. Electrochem. Soc.* 131, 675 (1984).
12. K.K. Lew, L. Pan, T.E. Bogart, S.M. Dilts, E.C. Dickey, J.M. Redwing, Y. Wang, M. Cabassi, T.S. Mayer, and S.W. Novak, *Appl. Phys. Lett.* 85, 3101 (2004).
13. W. He, R. Solanki, J.F. Conley, and Y. Ono, *J. Appl. Phys.* 94, 3657 (2003).
14. J. Huo, R. Solanki, J.F. Freeouf, and J.R. Carruthers, *Nanotechnology* 15, 1848 (2004).
15. M. Hansen, *Constitution of Binary Alloys* (New York: McGraw-Hill, 1958), pp. 186–222.
16. S.M. Sze, *VLSI Technology*, 1st ed. (New York: McGraw-Hill, 1983).
17. M.S. Gudiksen, L.J. Lanhon, J. Wang, D.C. Smith, and C.M. Lieber, *Nature* 415, 617 (2002).
18. S.P. Murarka and M.C. Peckerar, *Electronic Materials: Science and Technology*, (Orlando, FL: Academic Press, 1989), pp. 127–132.
19. J.B. Xia and K.W. Cheah, *Phys. Rev. B: Condens. Matter Mater. Phys.* 55, 15688 (1997).
20. D.D.D. Ma, C.S. Lee, F.C.K. Au, S.Y. Tong, and S.T. Lee, *Science* 299, 1874 (2003).

Volu  
PAGE  
1509  
1513  
1518  
1523  
1530  
1537  
1543  
1547  
1552  
1558  
1566  
1571  
1581  
1593  
1600  
L7